

An Accelerating Flat FLRW Model with Observation Constraints and Dynamic Λ

G. K. Goswami^{1,*} and Anirudh Pradhan^{2,†}

¹*Department of Mathematics, Netaji Subhas University of Technology, New Delhi-110 078, India*

²*Centre for Cosmology, Astrophysics and Space Science (CCASS),
GLA University, Mathura-281 406, Uttar Pradesh, India*

In this paper, we explore power law solution of FLRW universe model that is associated with a variable cosmological term $\Lambda(t)$ as a linear function of $\frac{\ddot{a}}{a}$, $(\frac{\dot{a}}{a})^2$ and ρ . The model parameters were estimated on the basis of the four data sets: The Hubble 46 data, the Union 2.1 compilation data sets comprising of distance modulus of 580 SNIa supernovae at different redshifts, the Pantheon data set which contains Apparent magnitudes of 1048 SNIa supernovae at various redshifts and finally BAO data set of volume averaged distances at 5 redshifts. We employ the conventional Bayesian methodology to analyze the observational data and also the Markov Chain Monte Carlo (MCMC) technique to derive the posterior distributions of the parameters. The best fit values of Hubble parameter H_0 as per the four data sets are found as $61.53^{+0.453}_{-0.456}$, $69.270^{+0.229}_{-0.228}$, $78.116^{+0.480}_{-0.479}$, and $71.318^{+2.473}_{-2.283}$ respectively. Off late the present value of Hubble parameters H_0 were empirically given as 73 and 67.7 (km/s)/Mpc using distance ladder techniques and measurements of the cosmic microwave background. The OHD+BAO+Union and OHD+Pan+BAO+Union combined data sets provide the best fit Hubble parameter value H_0 as $67.427^{+0.197}_{-0.199}$ and $74.997^{+0.143}_{-0.145}$ respectively. The various geometrical and physical properties of the model were also investigated and were found in good agreements with observations.

PACS number: 98.80 cq, 98.80.-k, 04.20.Jb

Keywords: FLRW Model, Dynamical Cosmological constant Λ , Observational constraints

I. INTRODUCTION

The expansion of the universe is speeding up rather than slowing down, according to cosmic observations from supernova type Ia (SNeIa) [1–3], the Cosmic Microwave Background (CMB), large scale structure, weak lensing [4–7], Baryon Acoustic Oscillation and Spectroscopic Survey (BOSS) collaboration [8, 9], Planck collaboration [10] and Actacama Cosmology Telescope Polarimeters (ACTPol) collaboration [11]. It is a well-established fact that the majority of known gravitational phenomena can be explained by the successful general theory of relativity. Inclusion of cosmological constant in Einstein’s field equation gained importance as a positive cosmological constant is considered as a source of dark energy. Λ CDM cosmology [12, 13] is just the Eddington–Lemaître model with the difference that the cosmological constant term acts as a source of dark energy with equation of state $p_\Lambda = -\rho_\Lambda$. Latest works by Abazajian et al. and Sahni and Starobinsky [14, 15] support Λ CDM cosmology. A dynamic cosmological term $\Lambda(t)$ [16–20] continues to be of interest in contemporary cosmology theories because it provides a natural solution to the cosmological constant problem. Significant observational evidence points to the finding of either Λ or a component of the universe’s material content that behaves similarly to Λ and fluctuates slowly with time and space. There is currently strong evidence from a variety of observations that the cosmos has a non-zero cosmological term [21]. A cosmological term in the context of quantum field theory is equivalent to the vacuum’s energy density. It has been suggested that an excited vacuum fluctuation that sets off an inflationary expansion and super-cooling is what gave rise to the universe. The reheating that follows is caused by the release of trapped vacuum energy. A Λ , in the

* gk.goswami9@gmail.com

† pradhan.anirudh@gmail.com

context of quantum field theory, is equivalent to the vacuum's energy density. It has been suggested that an excited vacuum fluctuation that sets off an inflationary expansion and super cooling is what gave rise to the universe. The reheating that follows is caused by the release of trapped vacuum energy. The Λ acts as a repulsive force against the gravitational attraction between galaxies and is a measure of the energy of empty space. Since mass and energy are equal, if the Λ exists, the energy it represents counts as mass. Inflation could result from the energy of the Λ plus the stuff in the universe if it is large enough. The universe with a cosmological term would expand more quickly over time because to the force emanating from the cosmological term, in contrast to normal inflation [22]. Recent discussions by Dolgov [23–25], Sahni and Starobinsky [15], Ratra and Peebles [26], and others on the “problem” of the cosmological constant and cosmology with a time-varying cosmological constant have noted that the cosmological constant is a “constant” in the absence of any interaction with matter or radiation. Off late the authors[27–30] have developed accelerating universe model in f(R,T) gravity theory which shows transition from deceleration to acceleration and fits well on observational grounds.

In this paper, we attempted to model a physical spatially homogeneous and isotropic flat FLRW(Friedmann Lemaitre Robertson Walker) universe in GR(General relativity) by considering variable time dependent cosmological constant(CC) Λ . On the basic of Einstein Field equations for FLRW space time, the CC is assumed as linear function of $\frac{\ddot{a}}{a}$ describing acceleration, $\frac{\dot{a}^2}{a^2}$ which is square of Hubble parameter describing rate of expansion and the density ρ of the universe. On solving the field equations, we found that our model represents an accelerating Einstein-de Sitter universe. The model had undergone under the constraints of the four data sets. The Hubble 46 data set(OHD) describing Hubble parameter values at various redshifts(Table1 for references). Union 2.1 compilation data sets (Union) comprising of distance modulus of 580 SNIa supernovae at different redshifts [31]. The Pantheon data set(Pan) which contains Apparent magnitudes of 1048 SNIa supernovae at various redshifts [32, 33] and finally BAO data set(BAO) of volume averaged distances at 5 redshifts [34]. These data sets and their combinations were used to estimate the model parameters which also include H_0 the present value of Hubble parameters. The best fit values of Hubble parameter H_0 as per the four data sets described earlier are found as $61.53^{+0.453}_{-0.456}$, $69.270^{+0.229}_{-0.228}$, $78.116^{+0.480}_{-0.479}$ and $71.318^{+2.473}_{-2.283}$ respectively. While “early universe” techniques based on cosmic microwave background measurements agree on a value of 67.7 (km/s)/Mpc, the calibrated distance ladder techniques have converged on a value of H_0 approximately 73 (km/s)/Mpc. We also tried to achieve these values statistically by using combined data sets out of the four described earlier. We also worked out in finding the growth of matter and vacuum cosmological constant related energy densities of the universe. They do follow the increasing trend over redshifts which interprets that in the past the densities were high and over the time they are gradually decreasing due to the expansion of the universe. We have estimated that the present values ρ_0 and ρ_{Λ_0} of matter and Lambda vacuum densities are $3.244 * 10^{-30} gm/cm^3$ and $7.39 * 10^{-30} gm/cm^3$ respectively. The higher value of vacuum energy shows the dominance of this energy at present. We recall that this energy is responsible for the present acceleration of the universe as it creates negative anti gravitating pressure in the universe. Finally We have also developed the association of time over redshifts and estimated the present age of the universe. As per our model it is estimated as 21.7282 billion yrs which is considerably higher than that predicted by Lambda CDM model.

The paper is lined up in the following order. In the section 2, we present Einstein field equations for FLRW space time with variable cosmological constant. In this section we have also solved the field equations and obtained power law solutions for Hubble parameter, cosmological constant, matter and Lambda dominated energy densities. Section 3 has five subsections in which we have estimated model parameters H_0 , α , β and γ with the help of four data sets with short names OHD, Union, Pan and BAO. We have also estimated by combining these data sets to get more

better results which fit best with the observations. In section 4, we have obtained present values of matter, Lambda dominated vacuum energy density in proper units. In section 5, we have presented a expression to convert redshifts into time. we have also obtained present age of the universe. All sections are very well attached with figures and tables to look our findings at first sight. the last section contains some useful concluding remarks.

II. EINSTEIN FIELD EQUATIONS WITH VARIABLE COSMOLOGICAL CONSTANT $\Lambda(t)$ AND THEIR SOLUTIONS

We begin with the Einstein's field equations with cosmological constant

$$R_{\mu\nu} - \frac{R}{2}g_{\mu\nu} + \Lambda g_{\mu\nu} = 8\pi G T_{\mu\nu}, \quad (1)$$

where $R_{\mu\nu}$, R , $g_{\mu\nu}$, $T_{\mu\nu}$ are the Ricci tensor, Ricci scalar, metric tensor and energy-momentum tensor of the contents of the universe. The Friedmann-Robertson-Walker (FRW) metric is given by the line element

$$ds^2 = dt^2 - a^2(t) \left[\frac{dr^2}{1 - kr^2} + r^2(d\theta^2 + \sin^2\theta d\phi^2) \right], \quad (2)$$

where the curvature parameter $k = -1, 0, 1$ for open, flat and closed models of the universe, respectively and $a(t)$ is the scale factor which geometrically expands the universe over time. Since current observations from CMB detectors such as BOOMERanG, MAXIMA, DASI, CBI and WMAP confirm a spatially flat universe, $k = 0$. We consider universe to be filled with perfect fluid whose energy momentum tensor T^μ_ν is given as

$$T^\mu_\nu = (p + \rho)u^\mu u_\nu - p\delta^\mu_\nu, \quad (3)$$

where p and ρ are the pressure and matter-energy density of the perfect fluid. We have considered velocity vector $u^i = (1, 0, 0, 0)$, so that $u^i u_i = 1$. Velocity of light c is taken as 1. Solving Einstein's Field equations for FRW metric, we get following equations as

$$2\frac{\ddot{a}}{a} + \frac{\dot{a}^2}{a^2} - \Lambda = -8\pi G p, \quad (4)$$

$$\frac{\dot{a}^2}{a^2} - \frac{\Lambda}{3} = \frac{8\pi G}{3}\rho. \quad (5)$$

Here, dot denotes the time derivative. We want to develop an universe model with variable cosmological constant with a view to geometries gravity. It may result in getting an accelerating universe. The continuity equation of total fluid (matter with energy density ρ and vacuum energy density Λ) will be written as $\dot{\rho} + 3H(\rho + p) + \dot{\Lambda} = 0$, where ρ and Λ are varying with time. Here, we take for the time being $p = \gamma\rho$ and Λ denotes the varying vacuum energy satisfying $\omega_\Lambda = -1$. For $\gamma = 0$, one may have the pressure-less dust and for $\gamma = \frac{1}{3}$, the fluid will be radiation. For $\gamma = 1$, the stiff fluid may be visualized in $p = \gamma\rho$ relation. From the field equations, we infer that the dynamic cosmological term $\Lambda(t)$ is possibly a linear function of $\frac{\ddot{a}}{a}$, $(\frac{\dot{a}}{a})^2$ and ρ as follows:

$$\Lambda(t) = \alpha \frac{\ddot{a}}{a} + \beta \left(\frac{\dot{a}}{a} \right)^2 + 4\pi G \gamma \rho, \quad (6)$$

where α , β are arbitrary constants and γ is equation of state parameter of fluid. In the present analysis, we consider γ as a parameter and estimate its value from the observational data. On solving Eqs.(4), (5) and (6), we get the following expression for Hubble parameter H , ρ and Λ .

$$H(t) = \frac{H_0(-\gamma + \alpha(w+1) - 2)}{H_0(t-t_0)(w+1)(\beta + \alpha - 3) + (-\gamma + \alpha(w+1) - 2)}, \quad (7)$$

$$\rho(t) = \frac{H_0^2(\alpha + \beta - 3)(\alpha - \gamma + \alpha w - 2)}{4\pi G(\alpha - \gamma + H_0(t-t_0)(w+1)(\alpha + \beta - 3) + \alpha w - 2)^2}, \quad (8)$$

$$p(t) = \frac{\omega H_0^2(\alpha + \beta - 3)(\alpha - \gamma + \alpha w - 2)}{4\pi G(\alpha - \gamma + H_0(t-t_0)(w+1)(\alpha + \beta - 3) + \alpha w - 2)^2}, \quad (9)$$

where we have considered equation of state for perfect fluid as $p = w\rho$ and boundary condition is taken as $H = H_0$ when $t = t_0$.

We define energy parameters $\Omega_m(t)$ $\Omega_\Lambda(t)$ as follows:

$$\Omega_m(t) = \frac{8\pi G\rho(t)}{3H(t)^2} = \frac{2(\alpha + \beta - 3)}{3(\alpha - \gamma + \alpha w - 2)} \quad (10)$$

and

$$\Omega_\Lambda(t) = \frac{\Lambda(t)}{3H(t)^2} = \frac{\alpha - 2\beta - 3\gamma + 3\alpha w}{3(\alpha - \gamma + \alpha w - 2)} \quad (11)$$

So that from Eq. (5), we get

$$\Omega_m(t) + \Omega_\Lambda(t) = 1$$

It is verified that in our model too, the above energy relation holds good.

Integrating Eq.(7), we get expression for scale factor as follows:

$$a(t) = a_0 \left(\frac{-\gamma + H_0(w+1)(\alpha + \beta - 3)(t-t_0) + \alpha(w+1) - 2}{-\gamma + \alpha(w+1) - 2} \right)^{\frac{\alpha - \gamma + \alpha w - 2}{(w+1)(\alpha + \beta - 3)}}, \quad (12)$$

where boundary condition is taken as $a = a_0$ when $t = t_0$.

From Eqs.(7) and (12), we get a very familiar relation between Hubble parameter ' H ' and scale factor ' a ' as follows:

$$H(t) = H_0 \left(\frac{a_0}{a(t)} \right)^{\frac{(w+1)(\alpha + \beta - 3)}{-\gamma + \alpha(w+1) - 2}};$$

Now using one more familiar relation between scale factor a and redshift z as:

$$\left(\frac{a_0}{a(t)} \right) = 1 + z,$$

we get following a very important relation:

$$H(z) = H_0(1+z)^{\frac{(w+1)(\alpha+\beta-3)}{-\gamma+\alpha(w+1)-2}}; \quad (13)$$

The deceleration and jerk parameters q and j are obtained from the following formalism:

$$q := -\frac{a\ddot{a}}{\dot{a}^2} = \frac{d}{dt} \left(\frac{1}{H} \right) - 1 = \frac{d \ln H}{d \ln(1+z)} - 1, \quad (14)$$

and

$$j := \frac{a^2 \ddot{a}}{\dot{a}^3} = q(2q+1) - \frac{\dot{q}}{H} = q(2q+1) + \frac{dq}{d \ln(1+z)}. \quad (15)$$

In our model, these parameters are obtained as

$$q(z) = \frac{(w+1)(\alpha+\beta-3)}{-\gamma+\alpha(w+1)-2} - 1, \quad (16)$$

and

$$j(z) = \frac{(\beta+\gamma+(\beta-3)w-1)(\alpha+2\beta+\gamma+w(\alpha+2\beta-6)-4)}{(\alpha-\gamma+\alpha w-2)^2} \quad (17)$$

The density ρ of the universe and the cosmological constant Λ are obtained from Eqs.(10) and (11) as:

$$\rho(z) = \rho_c \frac{2(\alpha+\beta-3)(z+1)^{\frac{2(w+1)(\alpha+\beta-3)}{-\gamma+\alpha(w+1)-2}}}{3(\alpha-\gamma+\alpha w-2)} \quad (18)$$

and

$$\Lambda(z) = \frac{H_0^2(\alpha-2\beta-3\gamma+3\alpha w)(z+1)^{\frac{2(w+1)(\alpha+\beta-3)}{-\gamma+\alpha(w+1)-2}}}{\alpha-\gamma+\alpha w-2}, \quad (19)$$

where $\rho_c = \frac{3H_0^2}{8\pi G}$ is the critical density of the universe.

From these equations, we may obtained the present values of density and cosmological constant as

$$\rho_0 = \rho_c \frac{2(\alpha+\beta-3)}{3(\alpha-\gamma+\alpha w-2)}$$

and

$$\Lambda_0 = \frac{H_0^2(\alpha-2\beta-3\gamma+3\alpha w)}{\alpha-\gamma+\alpha w-2}.$$

So, we may express $\rho(z)$ and $\Lambda(z)$ in term of their present values as:

$$\rho(z) = \rho_0(z+1)^{\frac{2(w+1)(\alpha+\beta-3)}{-\gamma+\alpha(w+1)-2}} \quad (20)$$

and

$$\Lambda(z) = \Lambda_0(z+1)^{\frac{2(w+1)(\alpha+\beta-3)}{-\gamma+\alpha(w+1)-2}}. \quad (21)$$

These equations indicate that our model resembles Einstein-de Sitter universe with the difference that it describes accelerating universe with variable power law oriented cosmological constant provided that the deceleration constant given by Eq. (16) is positive. It will be seen from the latter sections that it is indeed positive. We may comment that our model present the current scenario of the accelerating universe.

III. ESTIMATIONS OF MODEL PARAMETERS α , β , γ , AND H_0 FROM VARIOUS AVAILABLE SNIA DATASETS, HUBBLE DATASETS AND BAO DATASETS.

A. Estimations of Model parameters from Hubble dataset.

We consider the Hubble parameter table [35] consisting of 46 data set of of observed values of H for various redshift in the range $0 \leq z \leq 2.36$ with possible error in observations.

We use this data set to estimate the model parameters $\alpha, \beta, \gamma, H_0$ in multiple ways. First we fit Hubble parameter function given by Eq. (13) to these data by method of least square and estimates model parameters. There after assuming these estimated values as initial guess, we use method of least χ^2 to make more refined estimations. Finally we carry Markov Chain Monte Carlo (MCMC) method to further refine the estimations by assuming χ^2 estimations as initial guess. We recall that χ^2 formula for Hubble function is as follows:

$$\chi^2(\alpha, \beta, \gamma, H_0) = \sum_{i=1}^{46} \frac{(H_{th}(z_i, \alpha, \beta, \gamma, H_0) - H_{ob}(z_i))^2}{\sigma(z_i)^2}. \quad (22)$$

Our estimations are shown in the following Table-2

Parameters	Least square Estimations	Least χ^2 Estimations	MCMC simulation Estimations
α	0.524	1.235 ± 0.024	1.234 ± 0.024
β	1.91	0.816 ± 0.024	0.817 ± 0.024
γ	0.908	0.685 ± 0.008	0.685 ± 0.008
H_0	59.609	61.537 ± 0.461	$61.53^{+0.453}_{-0.456}$

TABLE I: The best fit values of the model parameters α , β , γ and H_0 for the best fit $H(z)$ Hubble curve.

Now we substantiate our work by presenting various figures in form of plots. Fig.1 describes the Hubble parameter $H(z)$ versus redshifts z plot and error bar plot for the best fit values of model parameters α, β, γ and H_0 using methods of least square and minimum χ^2 function value. Fig.2 describes MCMC Simulation based estimations for model parameters α, β, γ and H_0 .

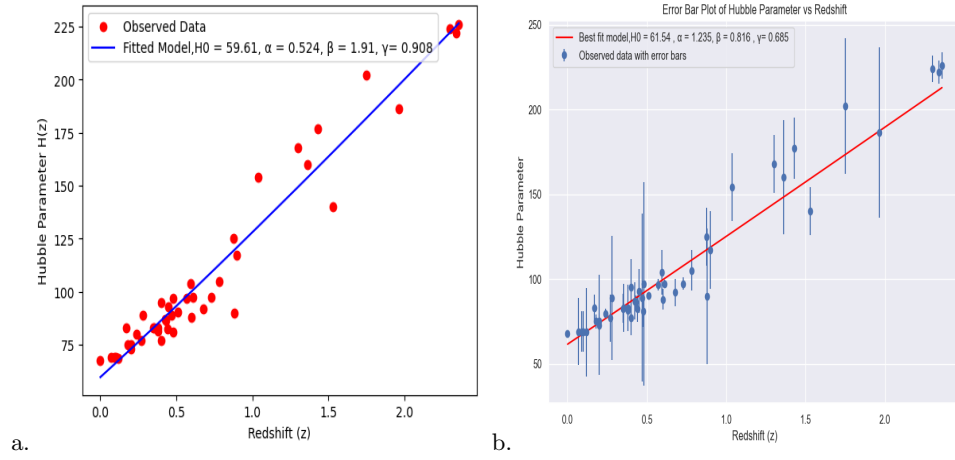


FIG. 1: The Hubble parameter $H(z)$ versus redshifts z Plot and Error bar Plot for the best fit values of model parameters α , β , γ and H_0 using method of least square and minimum χ^2 function value.

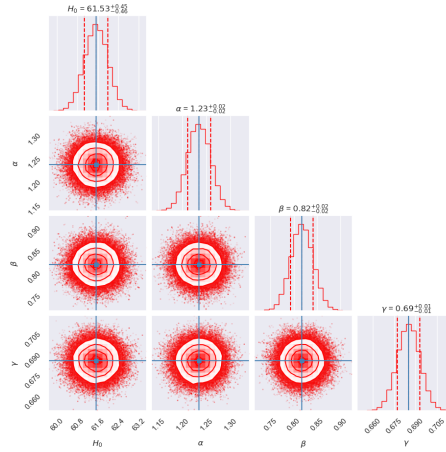


FIG. 2: Markov Chain Monte Carlo (MCMC) Simulation based estimations for Model parameters α , β , γ and H_0 and Corner plots for 36 Hubble data set.

B. Estimations of Model parameters from Supernova SNIa Union 2.1 Compilation 680 data set.

The Supernova SNIa Union 2.1 Compilation data set is comprised of 650 data set of Distance modulus of SNIa supernovae for various redshifts in the range $0 \leq z \leq 1.4$ associated with observational errors. The theoretical formula for distance modulus is given as:

$$\mu_{th}(z; h, \mathbf{params}) := 5 \log [D_L(z; \mathbf{params})] + \mu_0(h). \quad (23)$$

Here h is the Hubble constant in units of $100 \text{ km/s Mpc}^{-1}$, \mathbf{params} denotes the set of cosmological parameters of interest other than h . In our model params are α, β, γ .

$$\mu_0(h) := 5 \log \left(\frac{10^3 c / (\text{km/s})}{h} \right) = 42.38 - 5 \log h.$$

and

$$D_L(z; h, \mathbf{params}) = (1 + z) \int_0^z \frac{dz'}{H(z'; h, \mathbf{params})/H_0},$$

is the luminosity distance. We use Hubble function as per Eq.(13).

Like in sub section (a), we use union 2.1 data set to estimate the model parameters $\alpha, \beta, \gamma, H_0$ in multiple ways. First we fit distance modulus (m_u) function given by Eq.(23) to observational distance modulus (m_u) data by method of least square and estimates model parameters. There after assuming these estimated values as initial guess, we use method of least χ^2 to make more refined estimations. Finally we carry Markov Chain Monte Carlo (MCMC) method to further refine the estimations by assuming χ^2 estimations as initial guess. We recall that χ^2 formula for distance modulus (μ) is as follows:

$$\chi^2(\alpha, \beta, \gamma, H_0) = \sum_{i=1}^{580} \frac{(m_{bth}(z_i, \alpha, \beta, \gamma, H_0) - m_{bob}(z_i))^2}{\sigma(z_i)^2}. \quad (24)$$

Our estimations are shown in the following Table-3

Parameters	Least square Estimations	Least χ^2 Estimations	MCMC simulation Estimations
α	1.112	1.115 ± 0.03	0.987 ± 0.030
β	0.944	0.94 ± 0.03	0.961 ± 0.030
γ	0.943	0.941 ± 0.01	0.866 ± 0.01
H_0	68.694	69.273 ± 0.23	$69.270^{+0.229}_{-0.228}$

TABLE II: The best fit values of the model parameters α, β, γ and H_0 for the best fit distance modulus $\mu(z)$ curve.

Now we substantiate our work by presenting various figures in form of plots. Fig.4 describes the distance modulus $\mu(z)$ versus redshifts z Plot and Error bar Plot for the best fit values of model parameters α, β, γ and H_0 using methods of least square and minimum χ^2 function value. Fig.5 describes Markov Chain Monte Carlo (MCMC) simulation based estimations for Model parameters α, β, γ and H_0 .

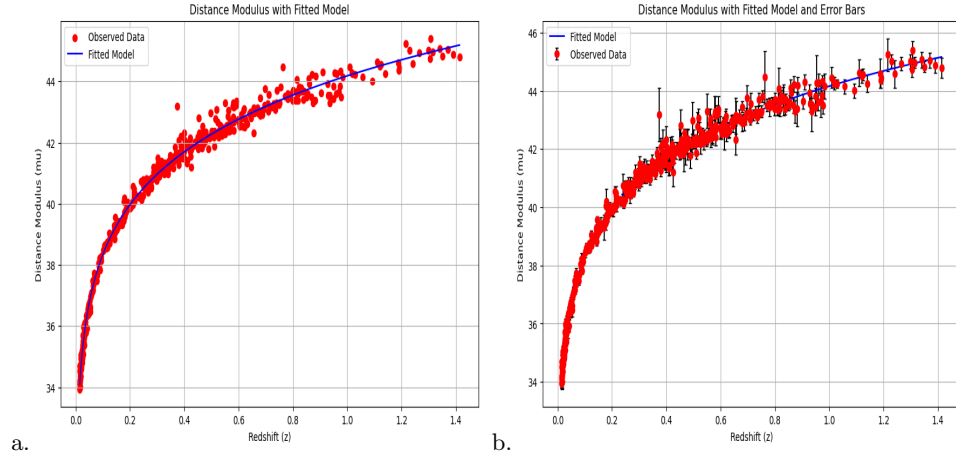


FIG. 3: The distance modulus (μ) versus redshifts z Plot and Error bar Plot for the best fit values of model parameters α , β , γ and H_0 using method of least square and minimum χ^2 function value . Estimated values are, $\alpha = 0.987 \pm 0.03$, $\beta = 0.961 \pm 0.03$, $\gamma = 0.866 \pm 0.01$ and 69.270 ± 0.23 .

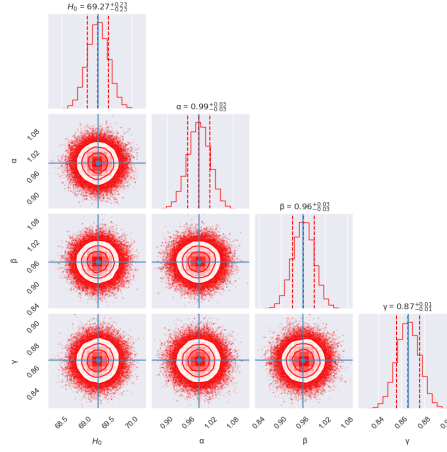


FIG. 4: Markov Chain Monte Carlo (MCMC) Simulation estimations for Model parameters α , β , γ and H_0 and Corner plots for Union 2.1 SNIa 680 data set .

C. Estimations of Model parameters from Supernova SNIa 1048 Pantheon data set.

The Supernova SNIa Pantheon data set is comprised of 1048 data set of Apparent magnitude (m_b) of SNIa supernovae for various redshifts in the range $0 \leq z \leq 2.24$, associated with observational errors. The theoretical formula for Apparent magnitude (m_b) is given as:

$$m_b = M + \mu(z)$$

where M is the absolute magnitude of the object and μ is the distance modulus. We recall that Type Ia supernovae are considered “standard candles” because they have a relatively uniform intrinsic brightness, which allows astronomers

to use them to measure distances accurately. The absolute magnitude of a typical Type Ia supernova at its peak brightness is approximately: Absolute Magnitude: $M = -19.09$ in the B- band(blue light)[12]

$$m_{bth}(z; h, \mathbf{params}) := 5 \log [D_L(z; \mathbf{params})] + m_{b0}(h). \quad (25)$$

Here h is the Hubble constant in units of $100 \text{ km/s Mpc}^{-1}$, \mathbf{params} denotes the set of cosmological parameters of interest other than h , in our model params are α, β, γ .

$$m_{b0}(h) := 5 \log \left(\frac{10^3 c / (\text{km/s})}{h} \right) - 19.09 = 23.29 - 5 \log h.$$

and

$$D_L(z; h, \mathbf{params}) = (1 + z) \int_0^z \frac{dz'}{H(z'; h, \mathbf{params})/H_0},$$

is the luminosity distance. We use Hubble function as per Eq.(13).

Like in sub section (a) and (b), we use Pantheon data set to estimate the model parameters $\alpha, \beta, \gamma, H_0$ in multiple ways. First we fit Apparent magnitude (m_b) function given by Eq.(23) to observational Apparent magnitude (m_b) data by method of least square and estimates model parameters. There after assuming these estimated values as initial guess, we use method of least χ^2 to make more refined estimations. Finally we carry Markov Chain Monte Carlo (MCMC) simulations method to further refine the estimations by assuming χ^2 estimations as initial guess. We recall that χ^2 formula for Apparent magnitude (m_b) is as follows:

$$\chi^2(\alpha, \beta, \gamma, H_0) = \sum_{i=1}^{1048} \frac{(m_{bth}(z_i, \alpha, \beta, \gamma, H_0) - m_{bob}(z_i))^2}{\sigma(z_i)^2}. \quad (26)$$

Our estimations are shown in the following Table-4

Parameters	Least square Estimations	Least χ^2 Estimations	MCMC simulation Estimations
α	1.145	1.522 ± 0.49	$1.521^{+0.488}_{-0.485}$
β	0.928	0.880 ± 0.49	$0.083^{+0.490}_{-0.479}$
γ	0.927	1.163 ± 0.49	$1.156^{+0.490}_{-0.479}$
H_0	77.713	78.122 ± 0.49	$78.116^{+0.480}_{-0.479}$

TABLE III: The best fit values of the model parameters α, β, γ and H_0 for the best fit Apparent magnitude $m_b(z)$ curve.

Now we substantiate our work by presenting various figures in form of plots. Fig.7 describes the distance modulus $\mu(z)$ versus redshifts z Plot and Error bar Plot for the best fit values of model parameters α, β, γ and H_0 using

methods of least square and minimum χ^2 function value. Fig.8 describes Markov Chain Monte Carlo (MCMC) Simulation based MCMC estimations for Model parameters α , β , γ and H_0 .

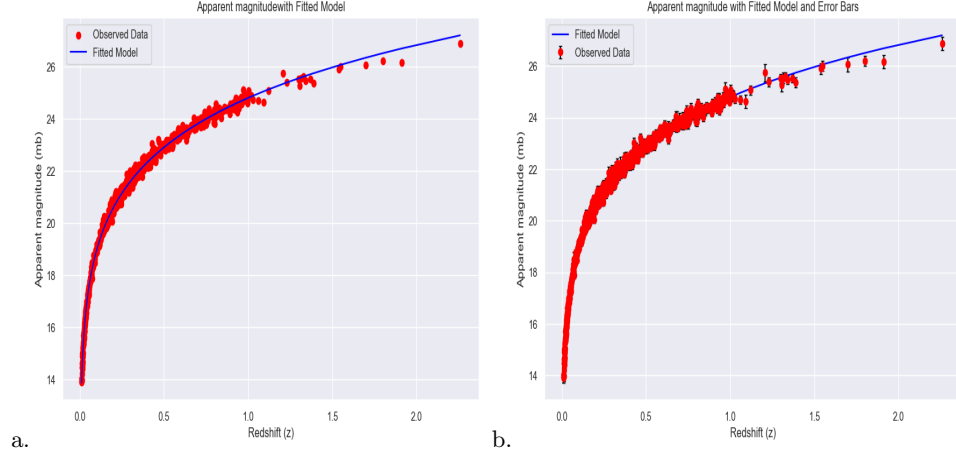


FIG. 5: The Apparent magnitude of least square and minimum χ^2 function value. Estimated values are $H_0 = 78.122 \pm 0.49$, $\alpha = 1.522 \pm 0.49$, $\beta = 0.880 \pm 0.49$, $\gamma = 1.163 \pm 0.49$.

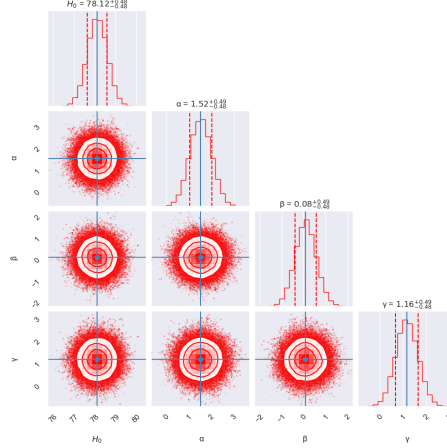


FIG. 6: Markov Chain Monte Carlo (MCMC) based estimations for Model parameters α , β , γ and H_0 and Corner plots for 1048 Pantheon data set.

D. Baryon Acoustic Oscillations Analysis:

BAO refers to the regular, periodic fluctuations in the density of visible baryonic matter (normal matter) of the universe, caused by acoustic waves in the early universe. BAO provides a "standard ruler" for length scale in cosmology. The scale of BAO is determined by the sound horizon at the time of recombination. By measuring the scale of BAO in the distribution of galaxies or in the Lyman-alpha forest of quasars, astronomers can determine distances across different epochs of the universe. BAO measurements help to trace the expansion history of the universe, complementing the information obtained from SNIa and CMB.

1. Key Parameters in BAO Analysis

Sound Horizon ($r_s(z)$): The distance that sound waves could travel in the early universe before recombination. This serves as the standard ruler for BAO measurements. It is defined as

$$r_s(a) = \int_0^a \frac{c_s da}{a^2 H(a)}.$$

It's typically about 150 mega parsecs (Mpc).

Angular Diameter Distance ($d_A(z)$): The distance derived from the angular size of BAO features at a given redshift. It is defined as

$$d_A(z) = c \int_0^z \frac{dz'}{H(z')}$$

Volume-Averaged Distance ($D_v(z)$): A combination of the angular diameter distance and the Hubble parameter, given by:

$$D_v(z) = \left(\frac{z d_A^2(z)}{H(z)} \right)^{\frac{1}{3}}$$

Ratio of Distances: The distance redshifts ratio is often used in BAO analysis to compare with theoretical predictions. It is given by:

$$d_z(z) = \frac{r_s(z^*)}{D_v(z)} \quad (27)$$

where $r_s(z^*)$ denotes the co-moving sound horizon at the time when photons decouple and z^* is the photons decoupling redshift. We consider $z^* = 1090$ for the analysis. In this work, we consider a sample of BAO distance measurements from different surveys such as SDSS(R)[36], the 6d F Galaxy survey [37], BOSS CMASS [38], and three parallel measurements from the Wiggle Z survey [39–42].

We consider the following observational data set for our analysis which are described as follows [34]:

$$\begin{aligned} z_{BAO} &= ([0.106, 0.2, 0.35, 0.44, 0.6, 0.73]) \\ d_z(z_{BAO}) &= ([30.95, 17.55, 10.11, 8.44, 6.69, 5.45]) \\ \sigma &= ([1.46, 0.60, 0.37, 0.67, 0.33, 0.31]) \end{aligned}$$

The χ_{BAO}^2 corresponding to BAO measurements is given by [34]

$$\chi_{BAO}^2(\alpha, \beta, \gamma, H_0) = X^T C^{-1} X, \quad (28)$$

where,

$$X = \begin{bmatrix} \frac{d_A(z^*)}{D_v(0.106)} - 30.84 \\ \frac{d_A(z^*)}{D_v(0.35)} - 10.33 \\ \frac{d_A(z^*)}{D_v(0.57)} - 6.72 \\ \frac{d_A(z^*)}{D_v(0.44)} - 8.41 \\ \frac{d_A(z^*)}{D_v(0.6)} - 6.66 \\ \frac{d_A(z^*)}{D_v(0.73)} - 5.43 \end{bmatrix} \quad (29)$$

and C^{-1} is the inverse of the covariance matrix given by [34]

$$C^{-1} = \begin{bmatrix} 0.52552 & -0.03548 & -0.07733 & -0.00167 & -0.00532 & -0.0059 \\ -0.03548 & 24.9707 & -1.25461 & -0.02704 & -0.08633 & -0.09579 \\ -0.07733 & -1.25461 & 82.9295 & -0.05895 & -0.18819 & -0.20881 \\ -0.00167 & -0.02704 & -0.05895 & 2.9115 & -2.98873 & 1.43206 \\ -0.00532 & -0.08633 & -0.18819 & -2.98873 & 15.9683 & -7.70636 \\ -0.0059 & -0.09579 & -0.20881 & 1.43206 & -7.70636 & 15.2814 \end{bmatrix} \quad (30)$$

We explain that the ratio $d_z(z)$ is in fact function of model parameters $\alpha, \beta, \gamma, H_0$. The same is true for χ^2 function also. So we use it to estimate our model parameters as we did in previous sections. We presents our results in the form of following table-5 and figures 10, 11 & 12.

Parameters	Least square Estimations	Least χ^2 Estimations	MCMC simulation Estimations
α	1.456	1.46 ± 0.020	$1.454^{+0.974}_{-0.992}$
β	1.556	1.56 ± 0.020	$1.574^{+0.960}_{-1.003}$
γ	1.899	1.90 ± 0.01	$1.920^{+0.582}_{-0.627}$
H_0	71.386	71.39 ± 1	$71.318^{+2.473}_{-2.283}$

TABLE IV: The best fit values of the model parameters α, β, γ and H_0 for the best fit distance ratio d_z curve.

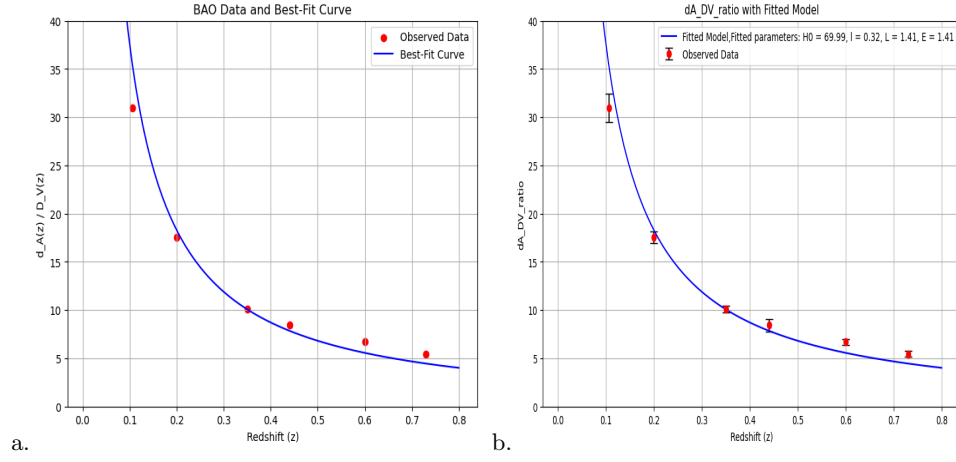


FIG. 7: The distance ratio d_z versus redshifts best fit plots on the basis of least square and minimum χ^2 function value. Estimated values are $H_0 = 65 \pm 1$, $\alpha = 0.11 \pm 0.020$, $\beta = 0.41 \pm 0.020$, $\gamma = 0.91 \pm 0.01$.

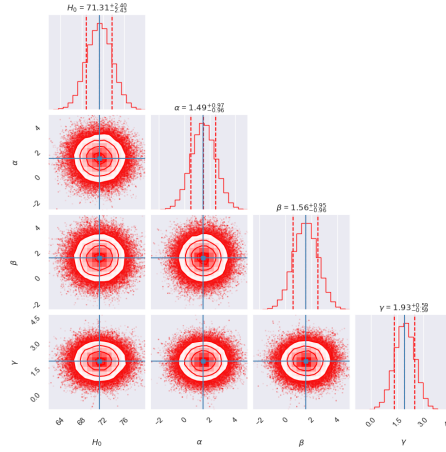


FIG. 8: Markov Chain Monte Carlo (MCMC) Simulation based estimations of Model parameters α , β , γ and H_0 and Corner plots for distance ratio d_z function.

E. Estimations of Model parameters from the combined data sets out of OHD, BAO, Pantheon and Union2.1 Compilation :

In this section, we continue our estimations of model parameters a , β , γ and H_0 with the help of combined data sets formed out of OHD, BAO, Pantheon and Union2.1 Compilation. For this we construct a combined χ^2 function by adding individual χ^2 function. For example suppose we want to combine OHD, BAO and Pantheon data sets then our combined chi square function will be as follows:

$$\chi^2_{OHD+PAN+BAO}(\alpha, \beta, \gamma, H_0) = \chi^2_{OHD}(\alpha, \beta, \gamma, H_0) + \chi^2_{PAN}(\alpha, \beta, \gamma, H_0) + \chi^2_{BAO}(\alpha, \beta, \gamma, H_0) \quad (31)$$

By minimizing the above function on giving proper initial values and ranges of model parameters, we estimate model parameters for combined data sets(CDS). We present the following table (VI) which displays estimated results for various CDS.

Parameters	OHD+UNION	OHD+BAO+Union	OHD+Pan+BAO+Union
H_0	$67.4^{+0.206}_{-0.205}$	$67.427^{+0.197}_{-0.199}$	$74.997^{+0.143}_{-0.145}$
α	0.973 ± 0.019	0.973 ± 0.013	1.364 ± 0.011
β	0.9 ± 0.019	0.901 ± 0.014	0.885 ± 0.012
γ	0.673 ± 0.006	0.676 ± 0.005	1.01739356 ± 0.001

TABLE V: Estimated values of Model Parameters α , β , γ and H_0

Note that the above estimated values are based on carrying Markov Chain Monte Carlo simulations which further refine the estimations by minimum χ^2 . Now, we present the following Corner plots and Step number plots (Fig. 13) to show the results of MCMC simulations. The details have been given in the caption of each plot.

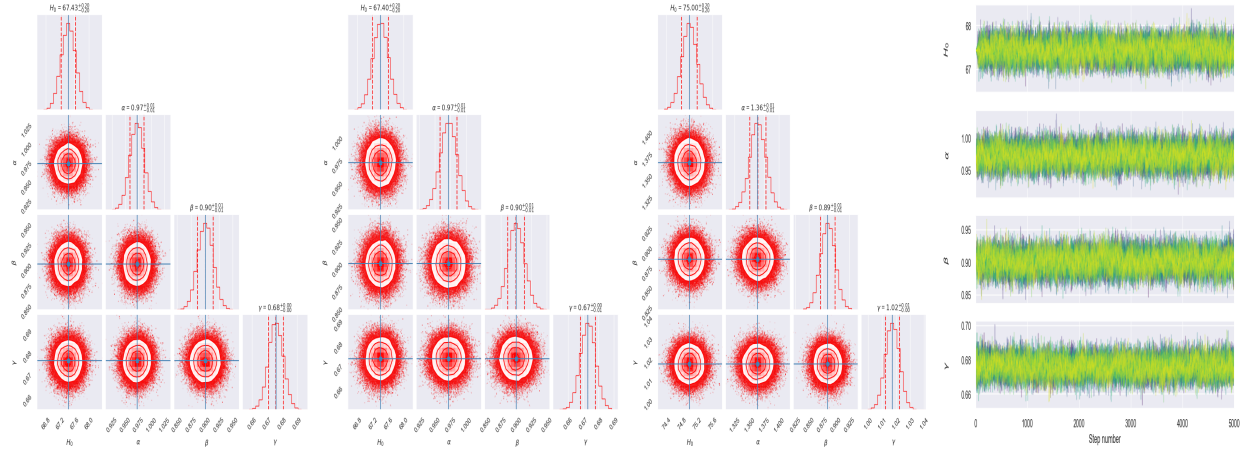


FIG. 9: Corner plots for Combined Hubble plus BAO plus Union 2.1 compilation and Hubble plus Union2.1 compilation data sets, based on Markov Chain Monte Carlo (MCMC) Simulation estimations of Model parameters α , β , γ and H_0 . The last two figures are Step numbers versus Model parameters α , β , γ and H_0 plots for combined data sets described earlier.

IV. HUBBLE TENSION

Various techniques have been employed in the 21st century to ascertain the Hubble constant. Utilizing calibrated distance ladder techniques, “late universe” observations have come to a consensus on a value of roughly 73 (km/s)/Mpc. A value of around 67.7 (km/s)/Mpc is agreed upon by “early universe” methodologies that rely on cosmic microwave background observations, which have been accessible since 2000. The investigation [43] is similar to the first number since it takes into account the variation in the expansion rate since the early universe. The estimated measurement

errors have decreased with improved methodologies, but the measured value range has not decreased, to the point that the disagreement is now extremely statistically significant. The ‘‘Hubble tension’’ refers to this disparity [44, 45]. We furnish the following list of present values of Hubble parameter H_0 obtained from latest surveys and projects.

Date published	Hubble constant (km/s)/Mpc	Observer	Citation	methodology
2022-02-08	$73.4^{+0.99}_{-1.22}$	Pantheon+	[46]	‘‘SN Ia distance ladder (+SHOES)’’
2022-06-17	$75.4^{+3.8}_{-3.7}$	T. de Jaeger et al.	[47]	‘‘Type II supernovae as standardisable candles’’
2021-12-08	73.04 ± 1.04	SHOES	[48]	‘‘Cepheids-SN Ia distance ladder’’ (HST+Gaia EDR3+‘‘Pantheon+’’).
2023-07-19	67.0 ± 3.6	Sneppen et al.	[49]	‘‘Blackbody spectra of the optical counterpart’’ of neutron-star mergers,
2022-12-14	$67.3^{+10.0}_{-9.1}$	S. Contarini et al.	[50]	‘‘Statistics of cosmic voids using BOSS DR12 data set’’
2023-07-13	68.3 ± 1.5	SPT-3G	[51]	‘‘CMB TT/TE/EE power spectrum’’.

TABLE VI: Latest H_0 Related Findings on the basis of Various Empirical Experiments and Observations

If we compare results of tables 6 with those of table 7, we find that our estimations of Hubble parameter H_0 are very much close to the observed values.

A. Present Density and the Present Cosmological constant:

We recall the following Equations for density of the universe and cosmological constant:

$$\rho(z) = \rho_c \frac{2(\alpha + \beta - 3)(z + 1)^{\frac{2(w+1)(\alpha+\beta-3)}{-\gamma+\alpha(w+1)-2}}}{3(\alpha - \gamma + \alpha w - 2)}$$

and

$$\Lambda(z) = \frac{H_0^2(\alpha - 2\beta - 3\gamma + 3\alpha w)(z + 1)^{\frac{2(w+1)(\alpha+\beta-3)}{-\gamma+\alpha(w+1)-2}}}{\alpha - \gamma + \alpha w - 2},$$

where $\rho_c = \frac{3H_0^2}{8\pi G}$ is the critical density of the universe.

From these equations and using tables (VI), we obtain the present values of density of the universe and that of cosmological constant. We also find Vacuum Energy of the universe which is defined as:

$$\rho_\Lambda = \frac{\Lambda c^2}{8\pi G}.$$

We note that $\frac{3c^2}{8\pi G} = 0.000189 * 10^{29} g/cm^3$.

The results are described in the following table (8).

Parameters	OHD+BAO+Union	OHD+Pan+BAO+Union
H_0	67.427	74.997
Ω_m	0.435453	0.305221
Ω_Λ	0.564547	0.694779
ρ_0	$0.373872 * 10^{-29} gm/cm^3$	$0.324389 * 10^{-29} gm/cm^3$
Λ_0	$8.06442 * 10^{-32} sec^{-2}$	$12.2783 * 10^{-32} sec^{-2}$
ρ_{Λ_0}	$4.85098 * 10^{-30} gm/cm^3$	$7.38578 * 10^{-30} gm/cm^3$

TABLE VII: Estimated values of Density of the Universe and Cosmological Constant

We also present the plot (Fig. 14) to describe variation of density over redshifts which is a increasing one, This shows that in the past the density of the universe was more and it is decreasing over time. We note that the redshift is proportion to the time.

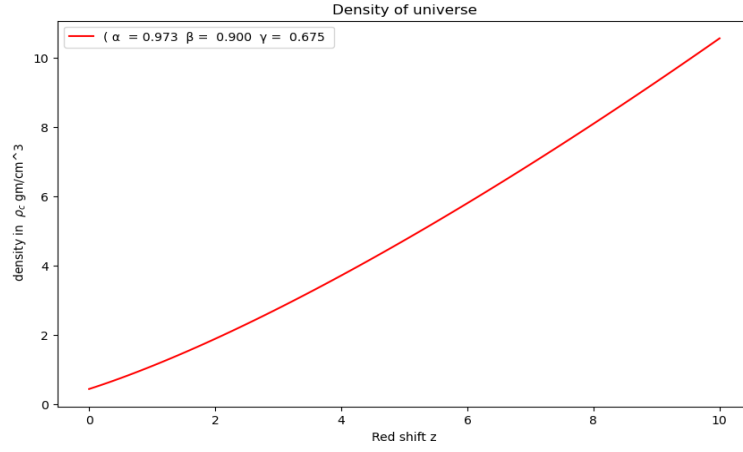


FIG. 10: Density versus redshift Plot

B. Conversion of Redshift into Time and Age of the Universe

We may get time in billion yrs in term of redshift from the following relation :

$$\frac{dz}{dt} = -(1+z)H(z)$$

This equation is integrated to yield the following relation ship between elapsed time $(t_0 - t_z)$ from present and redshift z :

$$(t_0 - t_z) = \int_0^z \frac{dz}{(1+z)H(z)} = \frac{(\gamma - \alpha + 2)}{(-3 + \alpha + \beta)H_0} ((1+z)^{\frac{-3+\alpha+\beta}{\gamma-\alpha+2}} - 1) \quad (32)$$

where t_0 is present time at $z = 0$ and t_z is the time at redshift z , so that $(t_0 - t_z)$ will be the elapsed time from present at the redshift z . We note that unit of Hubble parameter $H(z)$ Km/sec/Mps which is in fact a unit of reciprocal of time. We use following conversion formula to express $H(z)$ into reciprocal of billion yrs.

$$\frac{Mps}{km/sec} = 976.32 \text{ billionyrs.}$$

Now we present the following plot (Fig. 15) to show graphically redshift versus time relation:

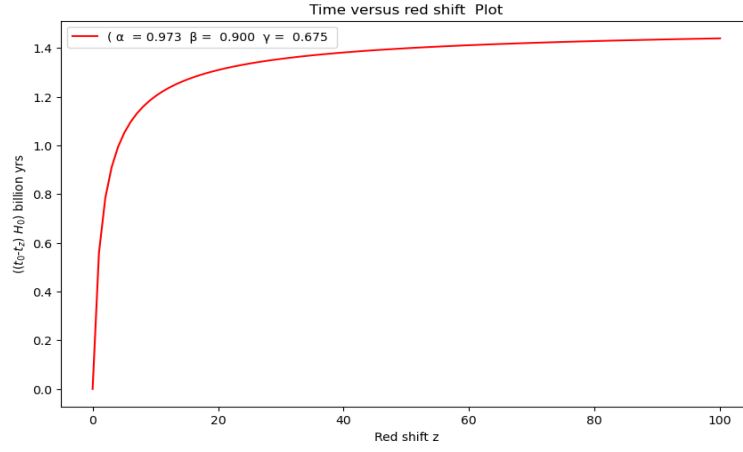


FIG. 11: Time versus redshift Plot

From this, we observe that there is an asymptote at $z = 1.4998$. This gives us age of the universe which is described in the table (9) as follows:

Parameters	OHD+BAO+Union	OHD+Pan+BAO+Union
H_0	$67.427^{+0.197}_{-0.199}$	$74.997^{+0.143}_{-0.145}$
α	0.973 ± 0.013	1.364 ± 0.011
β	0.901 ± 0.014	0.885 ± 0.012
γ	0.676 ± 0.005	1.017 ± 0.001
Age of The Universe	21.7282 billion yrs	22.7808 billion yrs

TABLE VIII: Age of the Universe as per estimations of model parameters

V. CONCLUSIONS

We developed a universe models of the FLRW space time that is associated with a variable cosmological term $\Lambda(t)$. For this the functional form of $\Lambda(t)$ is taken as $\alpha \frac{\ddot{a}}{a} + \beta (\frac{\dot{a}}{a})^2 + \gamma \rho$. We have been able to derive a power law solution for Hubble parameter $H(z)$, cosmological constant $\Lambda(z)$ and densities(matter and Lambda vacuum) of the universe in term of redshifts z and our model turns out to be a Einstein-de Sitter accelerating one. There are four model parameters $H_0, \alpha, \beta, \gamma$ which are were estimated on the basis of the four data sets. The Hubble 46 data set describing Hubble parameter values at various

redshifts, Union 2.1 compilation data sets comprising of distance modulus of 580 SNIa supernovae at different redshifts, The Pantheon data set which contains Apparent magnitudes of 1048 SNIa supernovae at various redshifts and finally BAO data set of volume averaged distances at 5 redshifts. We employ the conventional Bayesian methodology to analyze the observational data and also the Markov Chain Monte Carlo (MCMC) technique to derive the posterior distributions of the parameters. For MCMC analysis, we utilize the *emcee* package to determine the best-fit values of the model parameters. Along with this, we have also used technique of minimizing χ^2 function for parameter estimation. As a conclusion, we present our findings item wise as follows:

- we have carried out a detailed analysis of the universe expansion. Our investigation applies that the Hubble function envisages an increasing trend over redshift, which means that in the past the Hubble parameter was carrying high value and over the time it is gradually decreasing (See figs 1(a) and 1(b)). The best fit values of Hubble parameter H_0 as per the four data sets described earlier are found as $61.53^{+0.453}_{-0.456}$, $69.270^{+0.229}_{-0.228}$, $78.116^{+0.480}_{-0.479}$ and $71.318^{+2.473}_{-2.283}$ respectively.
- Off late the present value of Hubble parameters H_0 were empirically given as 73 and 67.7 (km/s)/Mpc using distance ladder techniques and measurements of the cosmic microwave background. We also tried to achieve these values statistically by using combined data sets out of the four described earlier. The OHD+BAO+Union and OHD+Pan+BAO+Union combined data sets provides the best fit Hubble parameter value H_0 as $67.427^{+0.197}_{-0.199}$ and $74.997^{+0.143}_{-0.145}$ respectively.
- We also worked out in finding the growth of matter and vacuum cosmological constant related energy densities of the universe. They do follow the increasing trend over redshift which interprets that in the past the densities were high and over the time they are gradually decreasing due to the expansion of the universe. We have estimated that the present values ρ_0 and ρ_{Λ_0} of matter and Lambda vacuum densities are $3.244 * 10^{-30} \text{ gm/cm}^3$ and $7.39 * 10^{-30} \text{ gm/cm}^3$ respectively. The higher value of vacuum energy shows the dominance of this energy at present. We recall that this energy is responsible for the present acceleration of the universe as it creates negative anti gravitating pressure in the universe.
- Lastly, we have calculated the universe's current age and established the relationship between time and redshift. Our model estimates the current age of the universe to be 21.7282 billion years, which is significantly more than the Λ -CDM model's prediction.
- In summary, the dynamical cosmological constant is a crucial concept in exploring the deeper nature of dark energy and how it governs the expansion and ultimate fate of the universe. It offers a more flexible framework than a static Λ , potentially solving several outstanding cosmological problems.

DECLARATION OF COMPETING INTEREST

The authors declare that they have no known competing financial interests or personal relationships that could have appeared to influence the work reported in this paper.

DATA AVAILABILITY

No data was used for the research described in the article.

ACKNOWLEDGMENTS

The IUCAA, Pune, India, is acknowledged by the author (A. Pradhan) for giving the facility through the Visiting Associateship programmes.

ORCID

Anirudh Pradhan: <https://orcid.org/0000-0002-1932-8431>

G. K. Goswami: <https://orcid.org/0000-0002-2178-6925>

REFERENCES

-
- [1] S. Perlmutter et al. [Supernova Cosmology Project Collab.], Measurements of the cosmological Parameters Omega and Lambda from the first 7 Supernovae at $z \geq 0.35$, *Astrophys. J.* **83** (1997) 565, arXiv: astro-ph/9608192.
 - [2] S. Perlmutter et al. [Supernova Cosmology Project Collab.], Discovery of a supernova explosion at half the age of the universe and its cosmological implications, *Nature* **91** (1998) 51, arXiv: astro-ph/9712212.
 - [3] S. Perlmutter et al. [Supernova Cosmology Project Collab.], Measurements of Omega and Lambda from 42 high-redshift supernovae, *Astrophys. J.* **17** (1999) 565, arXiv: astro-ph/9812133.
 - [4] G. Hinshaw, M. R. Nolte, C. L. Bennett et al., Three-Year Wilkinson Microwave Anisotropy Probe (WMAP) observations: Temperature analysis, *Astrophys. J. Supp.* **170** (2007) 288, arXiv:astro-ph/0603451.
 - [5] L. Page, G. Hinshaw, E. Komatsu et al., Three year Wilkinson Microwave Anisotropy Probe (WMAP) observations: Polarization analysis, *Astrophys. J. Supp.* **170** (2007) 335, arXiv:astro-ph/0603450
 - [6] C. L. Bennett et al., First year Wilkinson Microwave Anisotropy Probe (WMAP) observations: preliminary maps and basic results, *Astrophys. J. Suppl.* **148** (2003) 1–43, arXiv:astro-ph/0302207
 - [7] D. N. Spergel et al. [WMAP Collaboration], Three-year wilkinson microwave anisotropy probe (WMAP) observations: implications for cosmology, *Astrophys. J. Suppl. Ser.* **170** (2007) 377, arXiv:astro-ph/0603449
 - [8] L. Anderson et al. [BOSS Collaboration], The clustering of galaxies in the SDSS-III Baryon Oscillation Spectroscopic Survey: baryon acoustic oscillations in the Data Releases 10 and 11 Galaxy samples, *Month. Not. R. Astron. Soc.* **441** (2014) 24–62.
 - [9] E. Aubourg et al. [BOSS Collaboration], Cosmological implications of baryon acoustic oscillation measurements, *Phys. Rev. D* **92** (2015) 123516.
 - [10] C. Blake, S. Brough, M. Colless et al., The WiggleZ Dark Energy Survey: Joint measurements of the expansion and growth history at $z < 1$, *Mon. Not. R. Astron. Soc.* **425** (2012) 405.
 - [11] T. Louis, E. Grace, M. Hasselfield, et al., The Atacama Cosmology Telescope: two-season ACTPol spectra and parameters, *JCAP* **2017 (06)** (2017) 031.
 - [12] E. J. Copeland, M. Sami, S. Tsujikawa, Dynamics of dark energy, *Int. J. Mod. Phys. D* **15** (2006) 1753.
 - [13] ø. Grøn, and S. Hervik. Einstein’s general theory of relativity with modern applications in cosmology. Springer Publication (2007).
 - [14] K. Abazajian, J. K. Adelman-McCarthy, M. A. Agüeros, et al., The Second Data Release of the Sloan Digital Sky Survey, *Astron. J.* **128**, 502 (2004).
 - [15] V. Sahni and A. Starobinsky, The Case for a Positive Cosmological Lambda-term, *Int. J. Mod. Phys. D* **9** (2000) 373-443.
 - [16] R. G. Vishwakarma, Consequences on variable Lambda-models from distant Type Ia supernovae and compact radio sources. *Class. Quantum Gravity*, **18** (2021) 1159-1172.
 - [17] H. Azri, A. Bounames, Cosmological consequences of a variable cosmological constant model, *Int. J. Mod. Phys. D* **26** (2017) 1750060.
 - [18] H. Azri, A. Bounames, Geometrical origin of the cosmological constant, *Gen. Relat. Gravit.* **44** (2012) 2547-2561.
 - [19] M. Szydlowski, Cosmological model with decaying vacuum energy from quantum mechanics, *Phys. Rev. D* **91** (2015) 123538.

- [20] M. Koussour , N. Myrzakulov , J. Rayimbaev, Cosmological constraints on time-varying cosmological terms: A study of FLRW universe models with Λ CDM cosmology, *Advan. Space Resear.* **74** (2024) 1343-1351.
- [21] L. M. Krauss, M. S. Turner, The cosmological constant is back, *Gen. Relat. Gravit.* **27** (1995) 1137-1144.
- [22] K. Crowell, A death in the neighbourhood: Why did a giant red star turn orange before it died? Who stole its hydrogen? And what does it mean for the astronomers on the case? *New Scientist* 26 March, (1994).
- [23] A. D. Dolgov, in *The Very Early Universe*, eds. G. W. Gibbons, S. W. Hawking, S. T. C. Siklos, Cambridge University Press, Cambridge (1983).
- [24] A. D. Dolgov, M. V. Sazhin, Ya. B. Zeldovich, *Basics of Modern Cosmology*, Editions Frontiers (1990).
- [25] A. D. Dolgov, Higher spin fields and the problem of the cosmological constant, *Phys. Rev. D* **55** (1997) 5881.
- [26] B. Ratra and P. J. E. Peebles, Cosmological Consequences of a Rolling Homogeneous Scalar Field, *Phys. Rev. D* **37** (1988) 3406-3427.
- [27] A. Pradhan, G. Goswami, R. Rani, A. Beesham, An $f(R, T)$ gravity based FLRW model and observational constraints, *Astronomy and Computing* **44** (2023) 100737, arXiv:2210.15433[gr-qc].
- [28] A. Pradhan, G. K. Goswami, S. Krishnannair, The reconstruction of constant Jerk parameter with $f(R, T)$ gravity in Bianchi-I spacetime, *Eur. Phys. J. Plus* **138** (2023) 451, arXiv:2305.14400[gr-qc].
- [29] A. Pradhana, G. K. Goswami, A. Beesham, The reconstruction of constant Jerk parameter with $f(R, T)$ gravity, *JHEAP*, **38** (2023) 12–21, arXiv:2303.14136[gr-qc].
- [30] A. Pradhana, G. K. Goswami, A. Beesham, Reconstruction of an observationally constrained $f(R, T)$ gravity mode, *IJGMMP*, **20** (2023) 2350169, arXiv:2304.11616[gr-qc].
- [31] N. Suzuki et al., The Hubble space telescope cluster supernova survey V improving the dark energy constraints above $z > 1$ and building an early-type-hosted supernova sample, *Astrophys. J.* **746** (2012) 85–115.
- [32] D. Scolnic, D. Brout, A. Carr et al., The Pantheon+ analysis: the full data set and light-curve release, *Astrophys. J.* **938** (2022) 113.
- [33] D. D. M. Scolnic, D. O. Jones, A. Rest et al. The complete light-curve sample of spectroscopically confirmed SNe Ia from Pan-STARRS1 and cosmological constraints from the combined Pantheon sample, *Astrophys. J.* **859** (2018) 101, arXiv:1710.00845 [astro-ph.CO].
- [34] R. Giostri, M. V. dSantos, I. Waga, R. R. R. Reis, M. O. Calvao, B. L. Lago, From cosmic deceleration to acceleration: new constraints from SN Ia and BAO/CMB, *J. Cosmol. Astropart. Phys.*, **1203** 027 (2012).
- [35] Vinod Kumar Bhardwaj, Archana Dixit, Rita Rani, G.K. Goswami, and Anirudh Pradhan, An axially symmetric transitioning model with observational constraints, *Chin J Phys.* **80**, 261–274(2022)
- [36] N. Padmanabhan, X. Xu, D. J. Eisenstein, R. Scalzo, A. J. Cuesta, K. T. Mehta, E. Kazin, A 2 per cent distance to $z=0.35$ by reconstructing baryon acoustic oscillations - I. Methods and application to the Sloan Digital Sky Survey, *Mon. Not. Roy. Astron. Soc.* **427** (2012) 2132-2145, [arXiv:1202.0090 [astro-ph.CO]].
- [37] F. Beutler, C. Blake, M. Colless, D. H. Jones, L. Staveley-Smith, L. Campbell, Q. Parker, W. Saunders, F. Watson, The 6dF Galaxy Survey: Baryon Acoustic Oscillations and the Local Hubble Constant, *Mon. Not. Roy. Astron. Soc.* **416** (2011) 3017-3032, arXiv:1106.3366 [astro-ph.CO].
- [38] L. Anderson et al.[BOSS], The clustering of galaxies in the SDSS-III Baryon Oscillation Spectroscopic Survey: baryon acoustic oscillations in the Data Releases 10 and 11 Galaxy samples, *Mon. Not. Roy. Astron. Soc.* **441** (2014) 24-62 (2014), arXiv:1312.4877 [astro-ph.CO].
- [39] C. Blake, S. Brough, M. Colless, C. Contreras, W. Couch, S. Croom, D. Croton, T. Davis, M. J. Drinkwater, K. Forster et al., The WiggleZ Dark Energy Survey: Joint measurements of the expansion and growth history at $z < 1$, *Mon. Not. Roy. Astron. Soc.* **425** (2012) 405-414 (2012), arXiv:1204.3674 [astro-ph.CO].
- [40] C. Blake, E. Kazin, F. Beutler, T. Davis, D. Parkinson, S. Brough, M. Colless, C. Contreras, W. Couch, S. Croom et al., The WiggleZ Dark Energy Survey: mapping the distance-redshift relation with baryon acoustic oscillations, *Mon. Not. Roy. Astron. Soc.* **418** (2011) 1707-1724, arXiv:1108.2635 [astro-ph.CO].
- [41] W. J. Percival et al. [SDSS], Baryon Acoustic Oscillations in the Sloan Digital Sky Survey Data Release 7 Galaxy Sample, *Mon. Not. Roy. Astron. Soc.* **401** (2010) 2148-2168, arXiv:0907.1660 [astro-ph.CO].

- [42] D. J. Eisenstein et al. [SDSS], Detection of the Baryon Acoustic Peak in the Large-Scale Correlation Function of SDSS Luminous Red Galaxies, *Astrophys. J.* **633** (2005) 560-574, arXiv:astro-ph/0501171 .
- [43] W. L. Freedman, B. F. Madore, Progress in direct measurements of the Hubble constant, *JCAP* **11** (**2023**) (2023) 050, arXiv:2309.05618.
- [44] A. Mann, One Number Shows Something Is Fundamentally Wrong with Our Conception of the Universe – This fight has universal implications”, *Live Science*, Retrieved 26 August 2019.
- [45] E. D. Valentino, et al., In the realm of the Hubble tension—a review of solutions, *Class. Quant. Grav.* **38** (**15**) (2021) 153001, arXiv:2103.01183.
- [46] D. Brout, D. Scolnic, B. Popovic et al., The Pantheon+ analysis: Cosmological constraints, *The Astrophys. Jour.* **938** (2022) 110.
- [47] T. de Jaeger, L. Galbany, A. G. Riess, et al., A 5 per cent measurement of the Hubble-Lemaître constant from Type II supernovae, *MNRAS*, **514** (2022) 4620–4628.
- [48] A. G. Riess, W. Yuan, L. M. Macri, et al., A Comprehensive Measurement of the Local Value of the Hubble Constant with 1 km/s/Mpc Uncertainty from the Hubble Space Telescope and the SH0ES Team, *The Astrophys. Jour.* **934** (2022) L7.
- [49] S. Contarini, A. Pisani, N. Hamaus, F. Marulli, L. Moscardini, M. Baldi, The perspective of voids on rising cosmology tensions, *Astronomy & Astrophysics*, **682** (2023) A20.
- [50] A. Snepken, D. Watson, A. Bauswein, et al. Spherical symmetry in the kilonova AT2017gfo/GW170817, *Nature* **614** (2023) 436–439.
- [51] L. Balkenhol, D. Dutcher, M. Spurio et al. [SPT-3G Collaboration], Measurement of the CMB temperature power spectrum and constraints on cosmology from the SPT-3G 2018 TT, TE, and EE dataset, *Phys. Rev. D* **108** (2023) 023510.